Applied Microscopy
Korean Society of Microscopy

pISSN 2287-5123 · eISSN 2287-4445
http://dx.doi.org/10.9729/AM.2014.44.4.123

Silicene on Other Two-dimensional Materials: Formation of Heterostructure

Jung Hwa Kim, Zonghoon Lee*

School of Materials Science and Engineering, Ulsan National Institute of Science and Technology (UNIST) and Center for Multidimensional Carbon Materials, Institute for Basic Science (IBS), Ulsan 689-798, Korea

*Correspondence to:
Lee Z,
Tel: +82-52-217-2327
Fax: +82-52-217-2309
E-mail: zhlee@unist.ac.kr

Received December 24, 2014
Revised December 26, 2014
Accepted December 26, 2014

Silicene is one of the most interesting two-dimensional materials, because of not only the extraordinary properties similar to graphene, but also easy compatibility with existing silicon-based devices. However, non-existing graphitic-like structure on silicon and unstable free-standing silicene structure leads to difficulty in commercialization of this material. Therefore, substrates are essential for silicene, which affects various properties of silicene and supporting unstable structure. For maintaining outstanding properties of silicene, van der Waals bonding between silicene and substrate is essential because strong interaction, such as silicene with metal, breaks the band structure of silicene. Therefore, we review the stability of silicene on other two-dimensional materials for van der Waals bonding. In addition, the properties of silicene are reviewed for silicene-based heterostructure.

Key Words: Silicene, Two-dimensional materials, Heterostructure, Band gap, van der Waals

INTRODUCTION

Two-dimensional (2D) materials attract attentions with extraordinary properties, resulting from charge and heat transport confined in a plane (Balandin et al., 2008; Fuhrer et al., 2010). Among them, silicene, 2D silicon monolayer, is one of the most attractive materials, due to easy integration in current silicon based electronic devices (Kara et al., 2009; Aufray et al., 2010; De Padova et al., 2011). In 2009, silicene was proved as a stable structure which is a hexagonal honeycomb lattice with a buckled height around 0.44 Å, shown as Fig. 1A (Cahangirov et al., 2009; Ding & Ni, 2009; Jose & Datta, 2014). In contrast to other 2D materials such as boron nitride (BN), molybdenum disulfide (MoS_2) and phosphorene, silicene shares some of the outstanding properties of graphene, such as linear dispersion in the vicinity of Dirac points, forming a Dirac cone (Vogt et al., 2012; Quhe et al., 2014). Dirac cone makes the massless Dirac fermions near the Fermi level, which results in ultra-high carrier mobility, 10^5 $cm^2V^{-1}s^{-1}$, comparable to graphene (Shao et al., 2013). In addition, as size of silicene increases, reorganization energy decreases which makes silicene promising for devices, due to the structural relaxation in holes or electrons (Jose & Datta, 2011). The buckled silicene structure induces dispersion of electrons and opening band gap (Drummond et al., 2012; Jose & Datta, 2012; Ni et al., 2012), while graphene is not even under an external electric field or on a substrate (Quhe et al., 2012).

Band gap opening is a crucial requirement for current electronic devices. Various methods are utilized to open the band gap of silicene. At first, vertical electric field opens band gap by breaking the symmetry of silicone (Jose & Datta, 2011; Drummond et al., 2012; Ni et al., 2012; Houssa et al., 2013; Liu & Zhang, 2013; Song et al., 2013). The width of band gap

This research was supported by Nano Material Technology Development Program through the National Research Foundation of Korea (NRF) funded by the Ministry of Science, ICT and Future Planning (2012M3A7B4049807). This work was also supported by IBS-R019-D1.

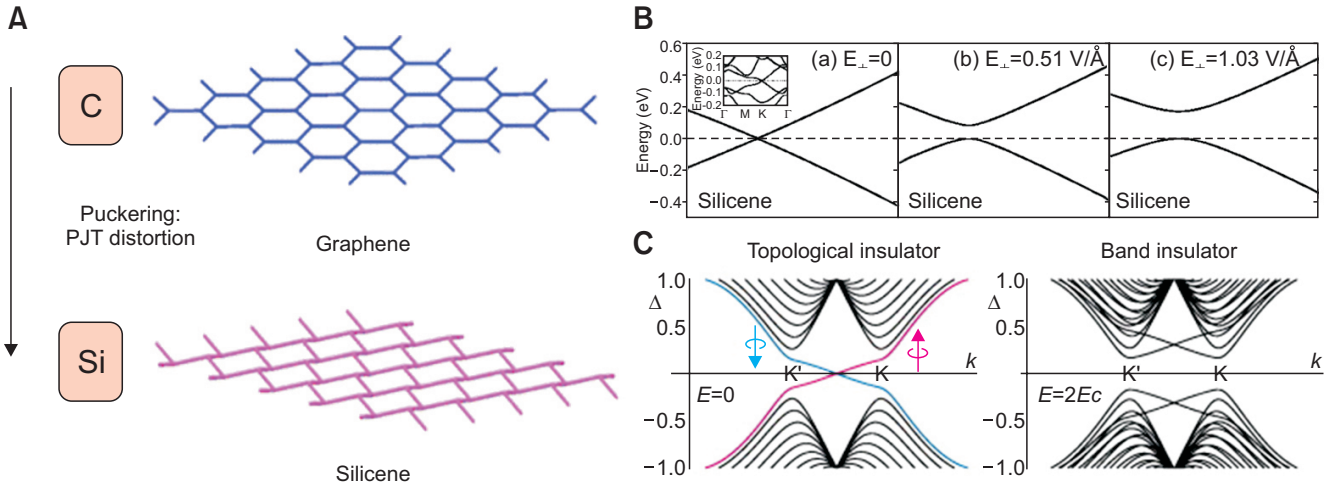

Fig. 1. (A) The structure of graphene and silicene. Puckered structure is derived from pseudo-Jahn-Teller (PJT) distortion. (B) Band structures of silicene around Fermi level at three different vertical electric fields (inset: band structures in the first Brillouin zone at vertical electric field=0, associated PJT). (C) One-dimensional energy bands for a silicene nanoribbon. In topological insulator, edge stages are crossed the gap in the band. There are two edge states since a nanoribbon has two edges (red and blue lines for the left and right edges). In insulator, all states are gapped, demonstrating that it is a band insulator. Fig. 1A and B are reprinted from Jose & Datta (2014) (*Accounts Chem. Res.* 47, 593-602) and Ni et al. (2012) (*Nano Lett.* 12, 113-118), respectively, with original copyright holder's permission. Fig. 1C is reprinted from Ezawa (2012b) (*New J. Phys.* 14, 033003).

and effective masses of electrons and holes in silicene can increase linearly with the external electric field, represented in Fig. 1B. Surprisingly, at low external electric field perpendicular to plane of silicene, it undergoes a transition between a topological insulator as shown in Fig. 1C, which conducts electrons only on the surface, and a simple band insulator, due to the induced quantum spin hall effect (Ezawa, 2012a, 2012b; Ezawa, 2013; Chang et al., 2014). Secondly, hydrogenation makes silicene wide band gap semiconductors (Jose & Datta, 2014). According to density functional theory calculations and molecular dynamics simulations, the band gap of silicene can be tuned by hydrogenation ratio (Liu et al., 2013). In addition, halogenation and lithiation are another methods to induce band gap in silicone (Voon & Guzman-Verri, 2014). Applied strain and acceptable temperature can control the width of band gap as well (Qin, 2014).

However, weak π-bonding of silicene causes considerably reactive silicene surface (Sahin & Peeters, 2013). It is derived from distance between silicon atoms and small energy difference between valence s and p orbital (Chavez-Castillo et al., 2012). Reactive surface of silicene adsorbs chemical species easily forming chemical bonds from the weak π-bonding to strong σ-bonding. When silicene surface reacts with transition metals, the product makes distinct properties such as planar structure with Ti and Ta, high stiffness with Nb and piezomagnet with Cr (Dzade et al., 2010). Because of sp^3 hybridization preference of silicene, physical exfoliation is impossible and layered silicene doesn't exist in nature. Therefore, to realize the utilization of silicene, the challenge for synthesis of silicene must be overcome. However, chemical deposition is also difficult because silicene prefers diamond structure. In addition, according to highly reactive surface, not only ultra-high vacuum system but also substrate for stabilizing sp^2 silicene should be necessary. In recent, there are many researches about fabrication of silicene on metal substrate, mainly Ag (Aufray et al., 2010; Gao & Zhao, 2012; Borensztein et al., 2014; Cahangirov et al., 2014; Chen & Weinert, 2014; Guo & Oshiyama, 2014; Johnson et al., 2014; Kawahara et al., 2014; Liu et al., 2014a, 2014b; Mahatha et al., 2014; Moras et al., 2014; Pflugradt et al., 2014a; Scalise et al., 2014; Shirai et al., 2014; Sone et al., 2014; Tchalala et al., 2014; Yuan et al., 2014). However the interaction between silicene and metal substrate degrades intrinsic properties of silicene. Since solid substrates for epitaxial growth of silicon are important requirements for fabrication of silicone (Meng et al., 2013), we will briefly review the proper 2D substrates for silicene fabrication, which don't hurt any excellent electronic properties and support silicene stably.

SYNTHESIS OF SILICENE

While silicon and carbon, which are the components of silicene and graphene, are in same column group 14 in periodic table, they are different in chemistry due to the different period, 3rd row and 2nd row, respectively. Energy differences between the valence s and p orbitals are 5.66 eV for silicon and 10.66 eV for carbon (Chavez-Castillo et al., 2012). As a result, silicon tends to use all three of p orbitals, resulting in sp^3 hybridization. In addition, the π-π overlap decreases from carbon to silicon due to the significant increase in atomic

distance as atomic number increases (Chavez-Castillo et al., 2012). It results in π bonding much weaker in silicon than carbon. Therefore, there is no silicon based layered structure in nature, due to preference of sp^3 hybridization, which means silicene cannot be made by exfoliation (Zhou et al., 2009). Silicene synthesis is also difficult because of the same reason. In recent, some studies have been discussed about synthesizing silicene on metal substrates (Lin & Ni, 2012; Kaltsas et al., 2014; Pan et al., 2014; Pflugradt et al., 2014b; Quhe et al., 2014). Ag is the most common substrates for silicene, because the moderate interaction between silicene and Ag can stabilize the sp^2 hybridized silicene. The Si/Ag system has distinct tendencies (Gao & Zhao, 2012). First, Si and Ag have phase separation with very low solubility of Si in bulk Ag. Second, the formation of Si takes place only on the top of Ag surface without any Si diffusion, due to the similar lattice constants. Third, the local tension in silicene during the growth process could be small due to the homogeneous interaction between Si and Ag.

SILICENE ON OTHER TWO-DIMENSIONAL MATERIALS

Above mentioned, although silicene has high carrier mobility from the massless Dirac fermion, zero band gap in pristine silicene prevents applying to devices such as field effect transistor (Cahangirov et al., 2009). Therefore, methods opening the band gap without degrading its electronic properties are very important for practical devices (Liu et al., 2013; Gao et al., 2014a). Recently, there are many researches about effect of substrates in silicene. Substrate under the silicene not only serves as mechanical supports for silicene but also makes the band gap opening of silicene without degrading its electronic properties (Sahin et al., 2013; Gao & Zhao, 2012). van der Waals (vdW) interaction between silicene and substrate makes the sublattices symmetry break, which opens the band gap. In other words, the different interface potential in silicene/substrate and different Coulomb fields in two sublattices in silicene make the charge redistribution and open a band gap (Chen et al., 2013; Lin et al., 2013). In addition, the high carrier mobility can be retained from vdW interaction, because this interlayer binding doesn't impair the π-bonding in sp^2 structure of silicene (Liu et al., 2013). It is also known that the magnitude of band gap can be controlled by the interlayer distance which is related to the magnitude of charge distribution in two sublattices. The smaller interlayer distance makes electron couplings more, breaks symmetry more and results in a larger band gap (Gao et al., 2014a). Likewise, there are various 2D substrates for silicene, which leads to heterostructure, shown as in Fig. 2 (Gao et al., 2014a, 2014b). 2D substrates can provide stable site for silicene and preserve intrinsic property of silicene. In addition, their heterostructures have potential for applying to flexible and tiny electronic devices. In this section, several heterostructures

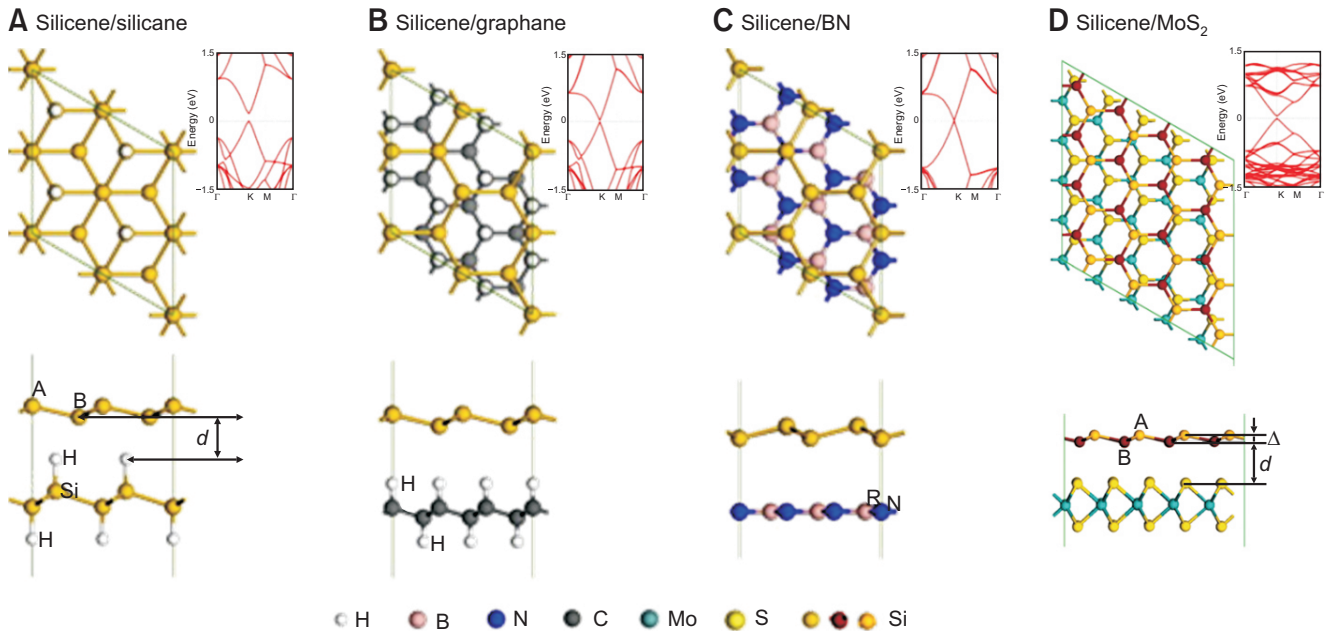

Fig. 2. The top and side views and corresponding band structures for silicene/silicane (A), silicene/graphane (B), silicene/boron nitride (BN) (C). The top view and corresponding band structure for silicene/molybdenum disulfide (MoS_2) (D). Fig. 2A-C are reprinted from Gao et al. (2014a) (*Chem. Phys. Lett.* 592, 222-226) with original copyright holder's permission. Fig. 2D is reprinted from Gao et al. (2014b) (*Phys. Chem. Chem. Phys.* 16, 11673-11678) with original copyright holder's permission.

composed of silicene and 2D substrates will be covered. Each heterostructures and property, mainly stability and band structure are discussed.

Silicene on BN

Hexagonal BN (h-BN) is an insulator with wide band gap. The cohesive energy between silicene and h-BN substrate is very weak about 0.07~0.09 eV per silicon atom, while about 0.5 eV per silicon atom on metal substrate (Kaloni et al., 2013). The vdW interaction, which is weak interaction between silicene and h-BN, does not affect to properties of silicene. Researchers predict quasi free-standing silicene could be realized in superlattice between silicene and h-BN due to the wide band gap of h-BN and weak vdW interaction (Ni et al., 2012; Kaloni et al., 2013a, 2013b; Li et al., 2013a; Liu et al., 2013; Kamal et al. 2014). The significant properties of free-standing silicene are preserved in quasi free-standing silicene, such as Dirac cone. However, vdW interaction is enough to hold silicene and BN together, forming silicene/BN moiré superstructure, shown as Fig. 3A (Li et al., 2013a). Fig. 3A shows superstructure (2,1/1,1) with a rotation angle 10.9°. Two sublattices of silicene with h-BN induce asymmetric interactions and lead to open band gap at the Dirac point of silicene. Interestingly, compared to graphene and h-BN superstructure, the width of band gap between silicene and h-BN system is rotation-independent (Li et al., 2013a). The band gap is tuned by the interlayer spacing between silicene and h-BN, represented in Fig. 3B. The indices of superstructure (2,1/1,1) and (3,0/2,0) are related to the rotation angle. The band gap changes effectively by interlayer distance, not by rotation angle.

The spatial distribution of charge densities proves the realization of quasi free-standing silicene (Kamal et al., 2014). There are two hybrid systems; one is graphite-like bulk system ($Si_{16}B_{18}N_{18}$) and the other is bi-layer ($Si_{16}B_9N_9$), shown in Fig. 3C and D, respectively. Charge densities are dominant in basal planes containing covalent bonds, which exist in one layer. Between adjacent layers, where vdW interactions are dominant, negligible amount of charge densities are present.

Compared to graphene, silicene has considerable spin-orbit coupling (SOC), because the atomic size of silicon is larger than that of carbon. Therefore, the combined effect of SOC and electric field is noteworthy (Kaloni et al., 2013a). According to various electric fields (E_z) at fixed SOC, different band structures are obtained as represented in (ii~iv) in Fig. 3D. As shown in Fig. 3D, the observed dependence of band gaps on the electric field with SOC is much stronger than without SOC. In addition, phase transitions are presented from a metal to a topological insulator and to a band insulator, in (ii~iv) in Fig. 3D.

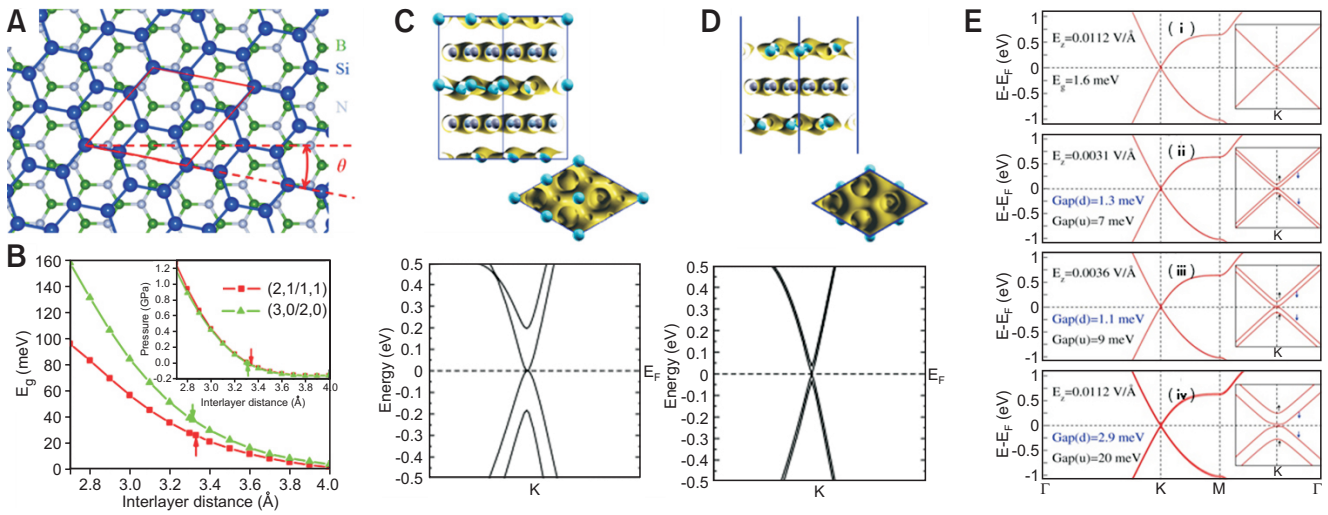

Fig. 3. (A) Superstructure of silicene on hexagonal boron nitride (h-BN) substrate with the rotation angle (θ) of 10.89°. The index of this superstructures is (2,1/1,1). The supercell containing 20 atoms is indicated by the rhombus. (B) Variation of the energy band gap of (2,1/1,1) and (3,0/2,0) silicene/BN superstructures as a function of interlayer distance between the two lattices. The pressure at different interlayer distances is plotted in the inset of this figure. The arrows indicate the equilibrium states. All the results are obtained from PBE+van der Waals calculations. Fig. 3C and D represent spatial charge density distributions of layered systems. The side and top view of hybrid graphite-like structures made up of silicene and boron nitride layers: bulk system ($Si_{16}B_{18}N_{18}$) for Fig. 3C and bi-layer ($Si_{16}B_9N_9$) for Fig. 3D. Corresponding band structures are below. (E) Electronic band structure of free-standing silicene in (i) with spin orbit coupling and E_z=0 or without spin orbit coupling and E_z=0.0112 V/Å, (ii~iv) with spin orbit coupling and different values of $E_z \neq 0$. Fig. 3A and B are reprinted from Li et al. (2013a) (*Phys. Lett. A* 377, 2628-2632) with original copyright holder's permission. Fig. 3C and D are reprinted from Kamal et al. (2014) (*Phys. Lett. A* 378, 1162-1169) with original copyright holder's permission. Fig. 3E is reprinted from Kaloni et al. (2013a) (*Sci. Rep-Uk.* 3, 3192) with original copyright holder's permission.

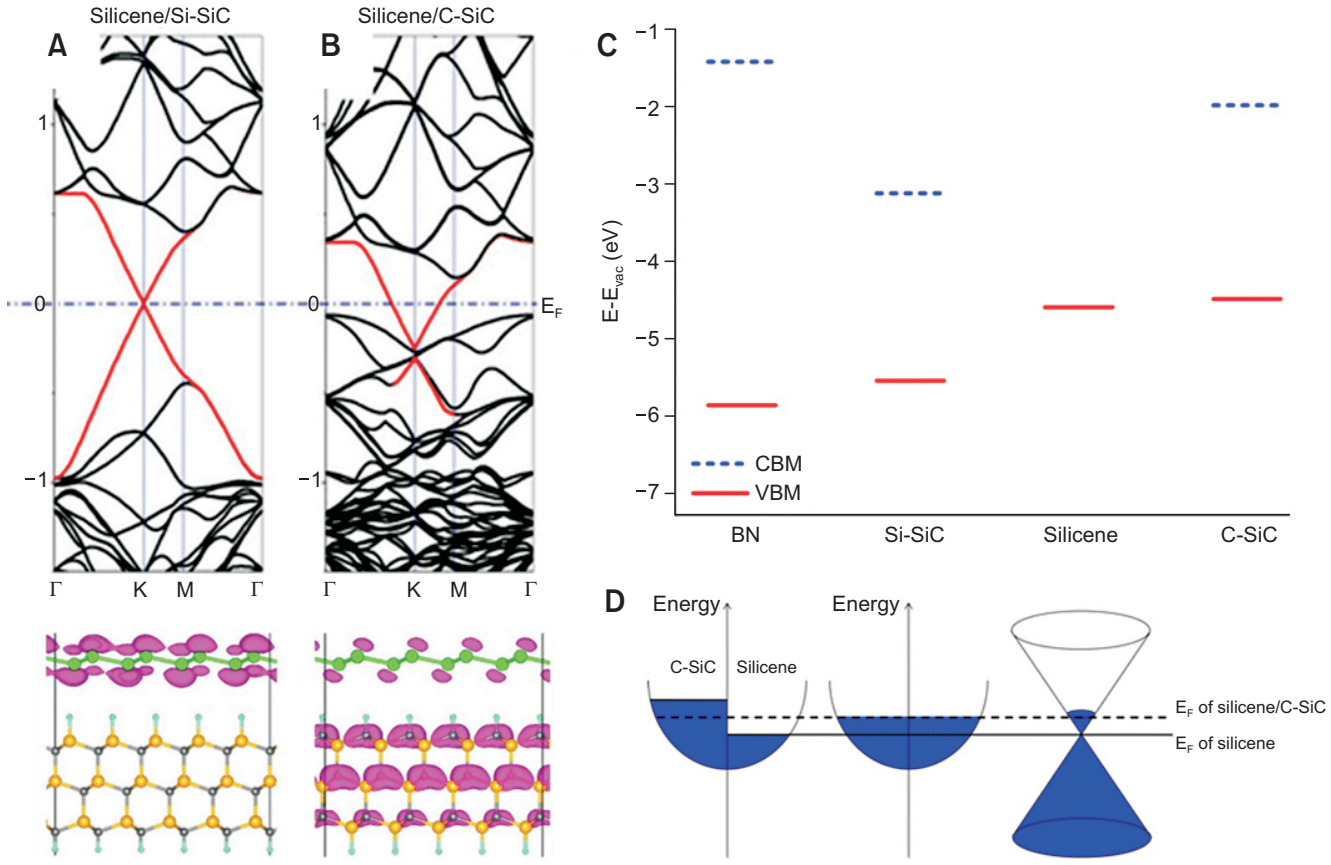

Fig. 4. Electron band structures of silicene/Si-SiC (A), silicene/C-SiC (B). The red lines highlight the π-bands of silicene in different configurations. Below diagram is partial charge densities for the π-bands near Fermi level (E_F~E_F -0.2 eV) (C) CBM and VBM of BN monolayer, Si-SiC substrate, silicene, and C-SiC substrate with respect to the vacuum level (set as zero energy). The values of CBM and VBM of silicene are exactly identical. (D) Schematic for the formation of metallic property for silicene/C-SiC hybrid system. Blue areas present the energy states occupied by electron. Left diagram states occupied by electron in isolated C-SiC and silicene, respectively; intermediate diagram states occupied by electron in the silicene/C-SiC hybrid system; last diagram states occupied by electron of silicene in the silicene/C-SiC hybrid system. Si-SiC, Si-terminated SiC(0001) surface; C-SiC, C-terminated SiC(0001) surface; CBM, conduction band minimum; VBM, valence band maximum; BN, boron nitride. Fig. 4 is reprinted from Liu et al. (2013) (*J. Phys. Chem. C* 117, 10353-10359) with original copyright holder's permission.

Silicene on Other Silicon Based Substrate

As shown in Fig. 4A and B, linear band dispersion of siliene near the Fermi energy is nearly preserved on the hydrogenated Si-terminated SiC(0001) surface (Si-SiC), while silicene on the hydrogenated C-terminated SiC(0001) surface (C-SiC) becomes metallic. For silicene/Si-SiC, partial charge densities in the energy range of E_F~E_F –0.2 eV concentrate on silicene, while for silicene/C-SiC, that distributes widely in silicene and C-SiC. It can be explained by work function. The valence band maximum (VBM) of silicene is slightly lower than the VBM of C-SiC, represented in Fig. 4C. When C-SiC is used as the substrate for silicene, two VBM energy levels are approaching certain interaction between silicene and C-SiC. As a consequence, some new electronic states arise between the two VBMs due to the strong electron coupling. On the other hands, in the case of silicene/Si-SiC and also silicene/BN, the VBM of silicene locates in the gap of the VBM of Si-SiC and BN, and that is far from its VBM. The electron coupling between silicene and those substrates is too weak to create any new electronic states. Consequently, the Fermi levels for silicene/BN and silicene/Si-Sic still cross the Dirac points of silicene. Thus, as represented in Fig. 3D, the Fermi level of the silicene/C-SiC hybrid system lies between the VBM of original silicene and the VBM of original C-SiC. Eventually, the Dirac cone of silicene is submerged under the Fermi level and slightly disturbed due to the electron coupling.

The silicene with chemically functionalized silicon ultrathin films can also open the band gap, preserving the Dirac cone, due to the inter-layer weak interactions, represented in Fig. 5A-D (Li et al., 2014a). Especially, silicene on ultrathin double Si with hydrogenation (DL-H) can control the band gap by external field and strain, as shown in Fig. 5E and F, respectively. Furthermore, hybrid armchair-silicane-silicene-nanoribbons and zigzag-silicane-nanoribbons have diverse

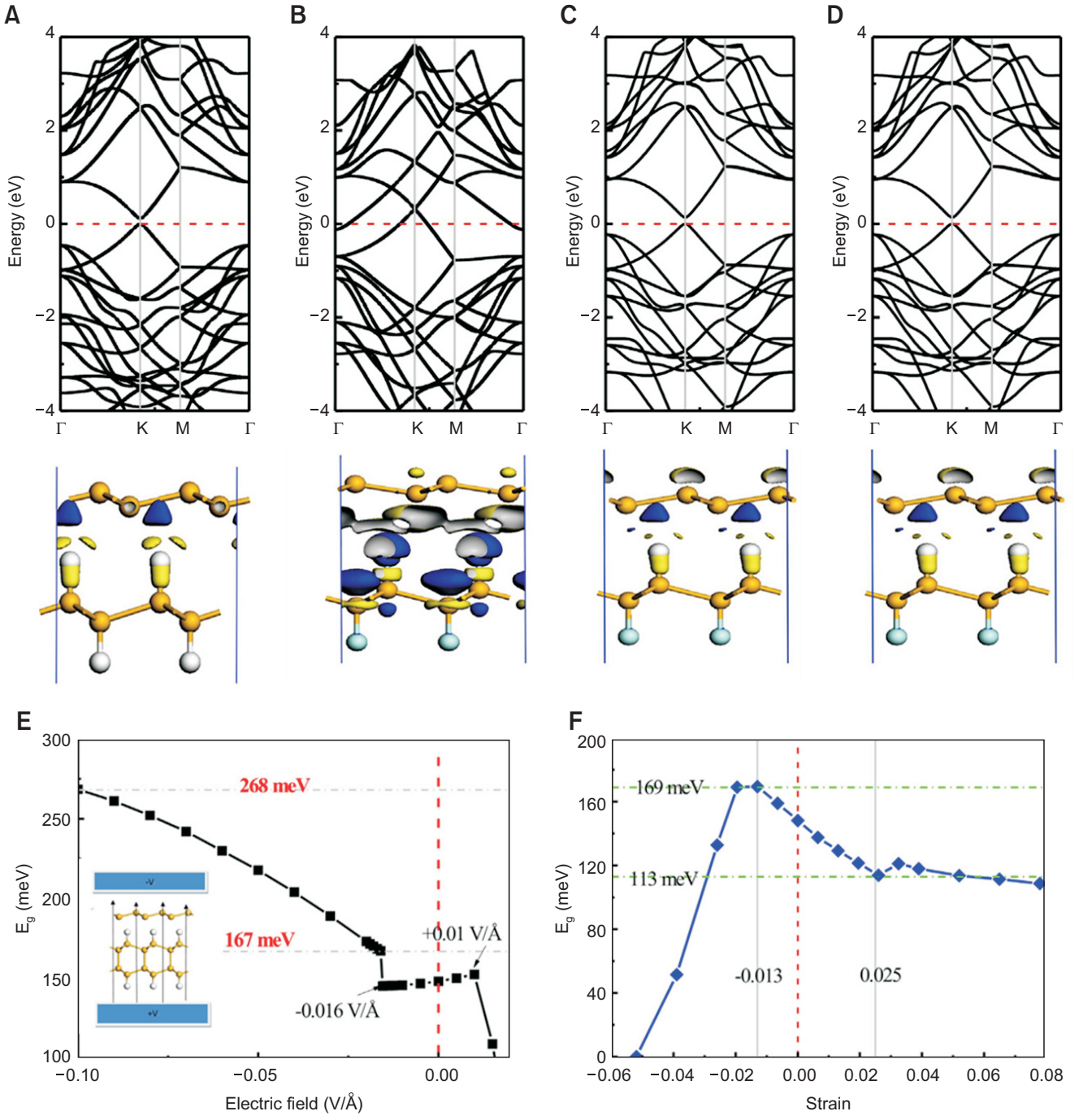

Fig. 5. Valence charge density distribution of bi-layers of Si/XSiX hetero-structures AB-1-Si/HSiH (A), AB-1-Si/FSiF (B), AB-1-Si/HSiF (C), and AA-2-Si/HSiH (D). The dot lines are Fermi level. The yellow and blue isosurfaces correspond to charge densities of 0.002 and 0.002 |e|/A^3, respectively. The variation of band gap of Si/double Si with hydrogenation as a function of the electric field intensity (E) and the strain (F). Fig. 5 is reprinted from Li et al. (2014a) (*Chem. Phys. Lett.* 609, 161-166) with original copyright holder's permission.

electronic and magnetic properties, which can be applied for devices (Li et al., 2014b).

Silicene on MoS_2

Because MoS_2 is a semiconductor with a considerable band gap, researchers pay attention to MoS_2 as a substrate for silicene (Ni et al., 2012; Li et al., 2013b; Liu et al., 2013; Chiappe et al., 2014; Gao et al., 2014a, 2014b; Jose & Datta, 2014; Li & Zhao, 2014; Li et al., 2014c). The most stable configuration in silicene/MoS_2 heterostructure is one Si

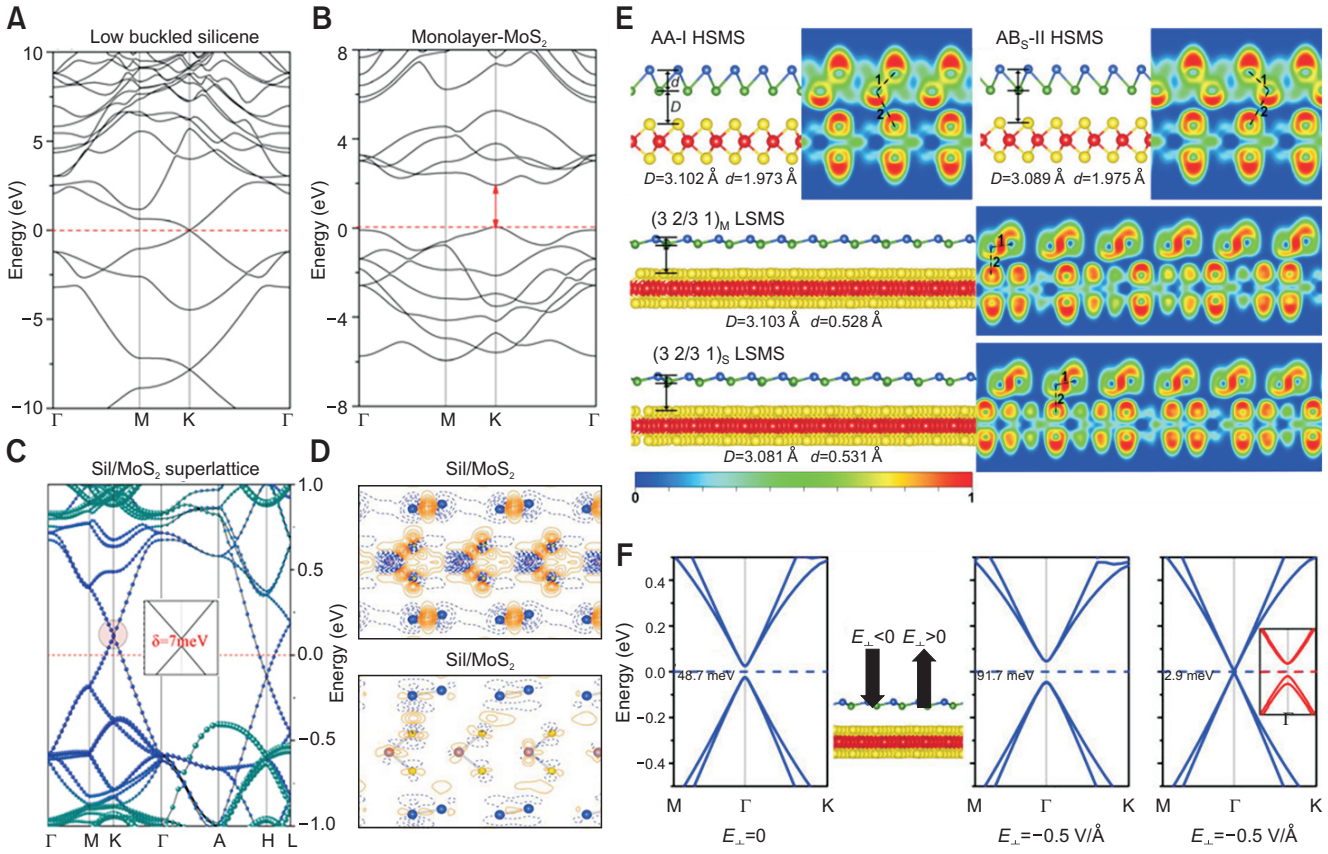

Fig. 6. Band structures of various materials. Low-buckled silicene (A), MoS_2 monolayer (B), and Sil/MoS_2 superlattices (C). The contributions from the silicene and MoS_2 layers to the band structures of the superlattices are shown with blue and green dots, respectively. The detailed band structures in the vicinity of the opened band gap are inserted. Red dashed lines represent the Fermi level. (D) Contour plots of the deformation charge density ($\Delta\rho_1$ and $\Delta\rho_2$). $\Delta\rho_1$ and $\Delta\rho_2$ on the planes perpendicular to the atomic layers and passing through Mo-S, Si-Si bonds in the superlattices are represented in upper and bottom image, respectively. The green/blue, purple, and yellow balls represent Si, Mo, and S atoms, respectively. Orange and blue lines correspond to $\Delta\rho>0$ and $\Delta\rho<0$, respectively. (E) Structure profiles of silicene on the MoS_2 substrate and their corresponding electron localization function profiles of AA-I HSMS, AB_S-II HSMS, $(3\ 2/3\ 1)_M$ LSMS, and $(3\ 2/3\ 1)_S$ LSMS. (F) Band structure of $(5\ 1/4\ 1)_M$ LSMS heterostructure. The energy at the Fermi level was set to zero. Brillouin zone folding moves the Dirac point from K to Γ point. Band structures of $(5\ 1/4\ 1)_M$ LSMS heterostructure in a vertical external electric field of E⊥=–0.5 V/Å and E⊥=0.5 V/Å. The direction of the external electric field is labeled in the figure. The enlarged view of the band lines at Γ point near the Fermi level is presented as the inset. The structural parameters of LSMS heterostructures classified by (n, m/p, q) and stacking patterns in origin (M and S). MoS_2, molybdenum disulfide; HSMS, high-buckled silicene on the MoS_2 substrate; LSMS, low-buckled silicene on the MoS_2 substrate. Fig. 6A-D are reprinted from Li et al. (2014c) (*Nanoscale Res. Lett.* 9, 110) with original copyright holder's permission. The place of inset in Fig. 6C is modified. Fig. 6E and F are reprinted from Li & Zhao (2014) (*J. Phys. Chem. C* 118, 19129-19138) with original copyright holder's permission.

atom is directly on S atom, and other Si atom is located above the hollow site of MoS_2 (Li et al., 2014c). In this heterostructure, binding energy (E_b) is 120.32 meV per Si atom, which is enough to hold silicene stably (Gao et al., 2014b). Corresponding interlayer distance, d, is 2.93 Å, which is larger than the sum of the covalent radii of the Si and S atoms, large interlayer distance leads to weak interactions between silicene and MoS_2, called as vdW interaction. Although linear band dispersions are preserved due to the weak interface interactions, a band gap is opened due to the broken symmetry by the intrinsic interface dipole (Gao et al., 2014b). Fig. 6C shows the effect of MoS_2 substrate on silicene, compared to pristine silicene and MoS_2 monolayer in Fig. 6A and B, respectively (Li et al., 2014c). The band structure of silicene on MoS_2 is like a simple sum of each band structure due to no effect each other. As shown in Fig. 6C, the band structure of silicene/MoS_2 has not only nearly linear band dispersion around the Dirac point, but also effective band gap, 7 meV. From this band structure on silicene/MoS_2 system, the partial density of states near the Fermi energy is dominated by π and π* states in silicene. Fig. 6D shows the contour plots of the deformation charge density (ρ_1) and charge transfer between the stacking layers in the superlattices (ρ_2) in silicene/MoS_2 system. The charge transfer in silicene/MoS_2 heterostructure is dominant within the silicene and the MoS_2 layers (intra-layer transfer). Some regions between silicene and MoS_2 layer (inter-layer transfer) have intermediate interactions. Compared to silicene/MoS_2

heterostructure, graphene/MoS_2 has much stronger inter-layer charge transfer, which means silicene/MoS_2 has much more than the vdW interactions between stacking layers (Li et al., 2014c). According to Gao et al. (2014b), induced band gap of silicene/MoS_2 is considerable 70 meV compared to the room temperature thermal scale (26 meV) and graphene/MoS_2 (nearly zero) (Ma et al., 2011), which result in improved on-off ratio. The band gap opening in silicene/MoS_2 is explained by plane-integrated electron density difference. Electron redistribution at an interface makes intrinsic interface dipole, and leads to open the band gap (Gao et al., 2014b). Silicene on MoS_2 forms silicene/MoS_2 heterostructure with high-buckled silicene and low-buckled silicene, called as HSMS and LSMS, respectively. In HSMS, it is stretched uniformly by about 16%, while low-buckled case is compressed by 0.72%. However, according to the electron localization function shown as Fig. 6E, silicene can remain in both cases without bond breaking, indicating covalent bonding represented in dotted line 1. The low-buckled case is more stable as represented in red. In the case of LSMS, likewise silicene/h-BN, the width of band gap is modulated by external electric field as represented in Fig. 6F, because external electric field changes the onsite energy difference between the two sublattices of silicene and change intrinsic interface dipole (Gao et al., 2014b; Li & Zhao, 2014). Recently, high-buckled silicene on bulk MoS_2 was synthesized using evaporation and was measured by scanning tunneling microscopy (STM) (Chiappe et al., 2014). Si nanosheet is grown epitaxially, and distinguished from the MoS_2 surface. Si ad-layer shows hexagonal rings with a three-fold symmetry and 3.2 Å lattice constant, compared to 3.8 Å lattice constant of free standing silicene. The shrinking of the Si lattice can be explained by the effect of lattice mismatch between the MoS_2 crystal (3.16 Å lattice constant) and the free standing silicene. The silicene structure is distinguished from the MoS_2 surface. The local electronic properties of Si nanosheet are dictated by the atomistic arrangement of the layer and unlike the MoS_2 substrate from gap-less density of states (Chiappe et al., 2014).

CONCLUSIONS

Silicene, analogue of graphene, has potential to integrate into current devices such as microprocessor chips and could lead to ultimate miniaturized and ultra-fast devices. So far, reasonable synthesis methods have not been established well. Synthesis of large area silicene is significant requirement for practical applications and appropriate substrate for stabilization of sp^2 bonding is needed against preference of sp^3 bonding in silicon. Although Ag is known as an excellent substrate for silicene, interactions between silicene and metallic Ag substrate degrade properties of silicene. According to many researches about various 2D substrates for silicene applications, 2D materials are proved that their appropriate interaction maintains intrinsic properties of silicene as well as opens band gaps effectively. Therefore, the reputation of silicon in electronic industry will be retained continuously if synthesis of silicene is achieved successfully on appropriate substrates.

CONFLICT OF INTEREST

No potential conflict of interest relevant to this article was reported.

REFERENCES

Aufray B, Kara A, Vizzini S, Oughaddou H, Leandri C, Ealet B, and Le Lay G (2010) Graphene-like silicon nanoribbons on Ag(110): a possible formation of silicene. *Appl. Phys. Lett*. **96**, 183102.

Balandin A A, Ghosh S, Bao W Z, Calizo I, Teweldebrhan D, Miao F, and Lau C N (2008) Superior thermal conductivity of single-layer graphene. *Nano Lett*. **8**, 902-907.

Borensztein Y, Prevot G, and Masson L (2014) Large differences in the optical properties of a single layer of Si on Ag(110) compared to silicene. *Phys. Rev. B* **89**, 245410.

Cahangirov S, Ozcelik V O, Xian L D, Avila J, Cho S, Asensio M C, Ciraci S, and Rubio A (2014) Atomic structure of the root 3 x root 3 phase of silicene on Ag(111). *Phys. Rev. B* **90**, 035448.

Cahangirov S, Topsakal M, Akturk E, Sahin H, and Ciraci S (2009) Two- and one-dimensional honeycomb structures of silicon and germanium. *Phys. Rev. Lett*. **102**, 236804.

Chang H R, Zhou J H, Zhang H, and Yao Y G (2014) Probing the topological phase transition via density oscillations in silicene and germanene. *Phys. Rev. B* **89**, 201411.

Chavez-Castillo M R, Rodriguez-Meza M A, and Meza-Montes L (2012) 2D radial distribution function of silicene. *Rev. Mex. Fis*. **58**, 139-143.

Chen L, Li H, Feng B J, Ding Z J, Qiu J L, Cheng P, Wu K H, and Meng S (2013) Spontaneous symmetry breaking and dynamic phase transition in monolayer silicene. *Phys. Rev. Lett* **110**, 085504.

Chen M X and Weinert M (2014) Revealing the substrate origin of the linear dispersion of silicene/Ag(111). *Nano Lett*. **14**, 5189-5193.

Chiappe D, Scalise E, Cinquanta E, Grazianetti C, van den Broek B, Fanciulli M, Houssa M, and Molle A (2014) Two-dimensional Si nanosheets with local hexagonal structure on a MoS2 surface. *Adv. Mater*. **26**, 2096-2101.

De Padova P, Quaresima C, Olivieri B, Perfetti P, and Le Lay G (2011) sp(2)-like hybridization of silicon valence orbitals in silicene nanoribbons. *Appl. Phys. Lett*. **98**, 081909.

Ding Y and Ni J (2009) Electronic structures of silicon nanoribbons. *Appl. Phys. Lett*. **95**, 083115.

Drummond N D, Zolyomi V, and Fal'ko V I (2012) Electrically tunable band gap in silicene. *Phys. Rev. B* **85**, 075423.

Dzade N Y, Obodo K O, Adjokatse S K, Ashu A C, Amankwah E, Atiso C D, Bello A A, Igumbor E, Nzabarinda S B, Obodo J T, Ogbuu A O, Femi O E, Udeigwe J O, and Waghmare U V (2010) Silicene and transition metal based materials: prediction of a two-dimensional piezomagnet. *J. Phys-Condens. Mat*. **22**, 375502.

Ezawa M (2012a) Topological phase transition and electrically tunable diamagnetism in silicene. *Eur. Phys. J. B* **85**, 363.

Ezawa M (2012b) A topological insulator and helical zero mode in silicene under an inhomogeneous electric field. *New J. Phys*. **14**, 033003.

Ezawa M (2013) Hexagonally warped Dirac cones and topological phase transition in silicene superstructure. *Eur. Phys. J. B* **86**, 139.

Fuhrer M S, Lau C N, and MacDonald A H (2010) Graphene: materially better carbon. *MRS Bull*. **35**, 289-295.

Gao J F and Zhao J J (2012) Initial geometries, interaction mechanism and high stability of silicene on Ag(111) surface. *Sci. Rep-Uk*. **2**, 861.

Gao N, Li J C, and Jiang Q (2014a) Bandgap opening in silicene: effect of substrates. *Chem. Phys. Lett*. **592**, 222-226.

Gao N, Li J C, and Jiang Q (2014b) Tunable band gaps in silicene-MoS2 heterobilayers. *Phys. Chem. Chem. Phys*. **16**, 11673-11678.

Guo Z X and Oshiyama A (2014) Structural tristability and deep Dirac states in bilayer silicene on Ag(111) surfaces. *Phys. Rev. B* **89**, 155418.

Houssa M, van den Broek B, Scalise E, Pourtois G, Afanas'ev V V, and Stesmans A (2013) An electric field tunable energy band gap at silicene/(0001) ZnS interfaces. *Phys. Chem. Chem. Phys*. **15**, 3702-3705.

Johnson N W, Vogt P, Resta A, De Padova P, Perez I, Muir D, Kurmaev E Z, Le Lay G, and Moewes A (2014) The metallic nature of epitaxial silicene monolayers on Ag(111). *Adv. Funct. Mater*. **24**, 5253-5259.

Jose D and Datta A (2011) Structures and electronic properties of silicene clusters: a promising material for FET and hydrogen storage. *Phys. Chem. Chem. Phys*. **13**, 7304-7311.

Jose D and Datta A (2012) Understanding of the buckling distortions in silicene. *J. Phys. Chem. C* **116**, 24639-24648.

Jose D and Datta A (2014) Structures and chemical properties of silicene: unlike graphene. *Accounts Chem. Res*. **47**, 593-602.

Kaloni T P, Tahir M, and Schwingenschlogl U (2013a) Quasi free-standing silicene in a superlattice with hexagonal boron nitride. *Sci. Rep-Uk*. **3**, 3192.

Kaloni T P, Gangopadhyay S, Singh N, Jones B, and Schwingenschlogl U (2013b) Electronic properties of Mn-decorated silicene on hexagonal boron nitride. *Phys. Rev. B* **88**, 235418.

Kaltsas D, Tsetseris L, and Dimoulas A (2014) Silicene on metal substrates: a first-principles study on the emergence of a hierarchy of honeycomb structures. *Appl. Surf. Sci*. **291**, 93-97.

Kamal C, Chakrabarti A, and Banerjee A (2014) Ab initio investigation on hybrid graphite-like structure made up of silicene and boron nitride. *Phys. Lett. A* **378**, 1162-1169.

Kara A, Leandri C, Davila M, Padova P, Ealet B, Oughaddou H, Aufray B, and Lay G (2009) Physics of silicene stripes. *J. Supercond. Nov. Magn*. **22**, 259-263.

Kawahara K, Shirasawa T, Arafune R, Lin C L, Takahashi T, Kawai M, and Takagi N (2014) Determination of atomic positions in silicene on Ag(111) by low-energy electron diffraction. *Surf. Sci*. **623**, 25-28.

Li G H, Tan J, Liu X D, Wang X P, Li F, and Zhao M W (2014b) Manifold electronic structure transition of hybrid silicane-silicene nanoribbons. *Chem. Phys. Lett*. **595**, 20-24.

Li L Y, Wang X P, Zhao X Y, and Zhao M W (2013a) Moire superstructures of silicene on hexagonal boron nitride: a first-principles study. *Phys. Lett. A* **377**, 2628-2632.

Li L Y and Zhao M W (2014) Structures, energetics, and electronic properties of multifarious stacking patterns for high-buckled and low-buckled silicene on the MoS2 substrate. *J. Phys. Chem. C* **118**, 19129-19138.

Li S, Wu Y F, Liu W, and Zhao Y H (2014a) Control of band structure of van der Waals heterostructures: silicene on ultrathin silicon nanosheets. *Chem. Phys. Lett*. **609**, 161-166.

Li X D, Mullen J T, Jin Z H, Borysenko K M, Nardelli M B, and Kim K W (2013b) Intrinsic electrical transport properties of monolayer silicene and MoS2 from first principles. *Phys. Rev. B* **87**, 115418.

Li X D, Wu S Q, Zhou S, and Zhu Z Z (2014c) Structural and electronic properties of germanene/MoS2 monolayer and silicene/MoS2 monolayer superlattices. *Nanoscale Res. Lett*. **9**, 110.

Lin C L, Arafune R, Kawahara K, Kanno M, Tsukahara N, Minamitani E, Kim Y, Kawai M, and Takagi N (2013) Substrate-induced symmetry breaking in silicene. *Phys. Rev. Lett*. **110**, 076801.

Lin X Q and Ni J (2012) Much stronger binding of metal adatoms to silicene than to graphene: a first-principles study. *Phys. Rev. B* **86**, 075440.

Liu H S, Gao J F, and Zhao J J (2013) Silicene on substrates: a way to preserve or tune its electronic properties. *J. Phys. Chem. C* **117**, 10353-10359.

Liu J J and Zhang W Q (2013) Bilayer silicene with an electrically-tunable wide band gap. *Rsc. Adv*. **3**, 21943-21948.

Liu Z L, Wang M X, Liu C H, Jia J F, Vogt P, Quaresima C, Ottaviani C, Olivieri B, De Padova P, and Le Lay G (2014a) The fate of the 2 root 3 x 2 root 3 R(30 degrees) silicene phase on Ag(111). *Apl. Mater*. **2**, 092513.

Liu Z L, Wang M X, Xu J P, Ge J F, Le Lay G, Vogt P, Qian D, Gao C L, Liu C H, and Jia J F (2014b) Various atomic structures of monolayer silicene fabricated on Ag(111). *New J. Phys*. **16**, 075006.

Ma Y D, Dai Y, Guo M, Niu C W, and Huang B B (2011) Graphene adhesion on MoS2 monolayer: an ab initio study. *Nanoscale* **3**, 3883-3887.

Mahatha S K, Moras P, Bellini V, Sheverdyaeva P M, Struzzi C, Petaccia L, and Carbone C (2014) Silicene on Ag(111): a honeycomb lattice without Dirac bands. *Phys. Rev. B* **89**, 201416.

Meng L, Wang Y L, Zhang L Z, Du S X, Wu R T, Li L F, Zhang Y, Li G, Zhou H T, Hofer W A, and Gao H J (2013) Buckled silicene formation on Ir(111). *Nano Lett*. **13**, 685-690.

Moras P, Mentes T O, Sheverdyaeva P M, Locatelli A, and Carbone C (2014) Coexistence of multiple silicene phases in silicon grown on Ag(111). *J. Phys-Condens. Mat*. **26**, 185001.

Ni Z Y, Liu Q H, Tang K C, Zheng J X, Zhou J, Qin R, Gao Z X, Yu D P, and Lu J (2012) Tunable bandgap in silicene and germanene. *Nano Lett*. **12**, 113-118.

Pan Y, Zhang L Z, Huang L, Li L F, Meng L, Gao M, Huan Q, Lin X, Wang Y L, Du S X, Freund H J, and Gao H J (2014) Construction of 2D atomic crystals on transition metal surfaces: graphene, silicene, and hafnene. *Small* **10**, 2215-2225.

Pflugradt P, Matthes L, and Bechstedt F (2014a) Unexpected symmetry and AA stacking of bilayer silicene on Ag(111). *Phys. Rev. B* **89**, 205428.

Pflugradt P, Matthes L, and Bechstedt F (2014b) Silicene on metal and metallized surfaces: ab initio studies. *New J. Phys*. **16**, 075004.

Qin R, Zhu W J, Zhang Y L, and Deng X L (2014) Uniaxial strain-induced mechanical and electronic property modulation of silicene. *Nanoscale Res. Lett*. **9**, 521.

Quhe R G, Yuan Y K, Zheng J X, Wang Y Y, Ni Z Y, Shi J J, Yu D P, Yang J B, and Lu J (2014) Does the Dirac cone exist in silicene on metal substrates? *Sci. Rep-Uk*. **4**, 5476.

Quhe R G, Zheng J X, Luo G F, Liu Q H, Qin R, Zhou J, Yu D P, Nagase S, Mei W N, Gao Z X, and Lu J (2012) Tunable and sizable band gap of single-layer graphene sandwiched between hexagonal boron nitride. *Npg. Asia Mater*. **4**, e6.

Sahin H and Peeters F M (2013) Adsorption of alkali, alkaline-earth, and 3d transition metal atoms on silicene. *Phys. Rev. B* **87**, 085423.

Sahin H, Sivek J, Li S, Partoens B, and Peeters F M (2013) Stone-Wales defects in silicene: formation, stability, and reactivity of defect sites. *Phys. Rev. B* **88**, 045434.

Scalise E, Cinquanta E, Houssa M, van den Broek B, Chiappe D, Grazianetti C, Pourtois G, Ealet B, Molle A, Fanciulli M, Afanas'ev V V, and Stesmans A (2014) Vibrational properties of epitaxial silicene layers on (111) Ag. *Appl. Surf. Sci*. **291**, 113-117.

Shao Z G, Ye X S, Yang L, and Wang C L (2013) First-principles calculation of intrinsic carrier mobility of silicene. *J. Appl. Phys*. **114**, 093712.

Shirai T, Shirasawa T, Hirahara T, Fukui N, Takahashi T, and Gasegawa S (2014) Structure determination of multilayer silicene grown on Ag(111) films by electron diffraction: evidence for Ag segregation at the surface (vol 89, 241403, 2014). *Phys. Rev. B* **90**, 039902.

Sone J, Yamagami T, Aoki Y, Nakatsuji K, and Hirayama H (2014) Epitaxial growth of silicene on ultra-thin Ag(111) films. *New J. Phys*. **16**, 095004.

Song Y L, Zhang S, Lu D B, Xu H R, Wang Z, Zhang Y, and Lu Z W (2013) Band-gap modulations of armchair silicene nanoribbons by transverse electric fields. *Eur. Phys. J. B* **86**, 488.

Tchalala M R, Enriquez H, Yildirim H, Kara A, Mayne A J, Dujardin G, Ali M A, and Oughaddou H (2014) Atomic and electronic structures of the (root 13 x root 13)R13.9 degrees of silicene sheet on Ag(111). *Appl. Surf. Sci*. **303**, 61-66.

Vogt P, De Padova P, Quaresima C, Avila J, Frantzeskakis E, Asensio M C, Resta A, Ealet B, and Le Lay G (2012) Silicene: compelling experimental evidence for graphenelike two-dimensional silicon. *Phys. Rev. Lett*. **108**, 155501.

Voon L C L Y and Guzman-Verri G G (2014) Is silicene the next graphene? *MRS Bull*. **39**, 366-373.

Yuan Y K, Quhe R G, Zheng J X, Wang Y Y, Ni Z Y, Shi J J, and Lu J (2014) Strong band hybridization between silicene and Ag(111) substrate. *Physica E* **58**, 38-42.

Zhou M, Li R S, Zhou J Y, Guo X S, Liu B, Zhang Z X, and Xie E Q (2009) Growth and characterization of aligned ultralong and diameter-controlled silicon nanotubes by hot wire chemical vapor deposition using electrospun poly(vinyl pyrrolidone) nanofiber template. *J. Appl. Phys*. **106**, 124315.